KSCE Journal of Civil Engineering (2018) 22(2):777-784
DOI 10.1007/s12205-017-1889-7

Structural Engineering
pISSN 1226-7988, eISSN 1976-3808
www.springer.com/12205

Blast Performance Evaluation of Structural Components under Very Near Explosion

Jinwon Shin* and Kyungkoo Lee**

Received November 23, 2016/Accepted April 5, 2017/Published Online June 14, 2017

Abstract

The single-degree-of-freedom (SDOF) analysis with elastic-plastic resistance is often used for design of protective structures subjected to blast loads. Several documents such as UFC 3-340-02 present design charts for the maximum responses of the elastic-plastic SDOF system. The SDOF design charts are available for far-field detonations but seldom for near-field detonations of high explosive in free air, noting that the focus of security design is the near-field. Further, the assumption of uniformly distributed load for the SDOF analysis may not be appropriate for the near-field detonations where blast pressure distribution varies significantly with distance and angle of incidence. In this paper, to resolve these issues, updated SDOF design charts including the response to the near-field detonations are suggested based on numerical calculations. These generated charts are verified with comparison to UFC 3-340-02 predictions and finite element analysis results of steel components. The recommendations and limitations for the utility of the SDOF design charts for blast assessment of steel components are provided with an emphasis on the near-field detonations.

Keywords: *blast performance evaluation, structural components, Near-field detonation, single-degree-of-freedom analysis, finite element method*

1. Introduction

The effects of air-blast loading are considered for design of protective structures such as mission-critical buildings, safety-related nuclear structures, and bridge. The typical practice for blast-resistant design involves either 1) numerical analysis using Computational Fluid Dynamics (CFD) and Finite Element Method (FEM), or 2) Single-degree-of-freedom (SDOF) analysis using empirical relationships. The latter is often preferred for blast-resistant design due to its simplicity, provided that this simplified method should be verified using the former approach.

The SDOF design method with elastic-plastic structural resistance has been developed since the 1950s in consideration of design on above-ground military facilities against the threat for thermonuclear detonations in the far field and is described in detail by Biggs (1952), Norris *et al.* (1959), TM 5-1300 (Department of the Army, Navy and Air Force, 1990), and UFC 3-340-02 (DoD, 2008). This SDOF design method uses blast loadings idealized with the Friedlander curve (e.g., Baker, 1973; Smith and Hetherington, 1994; Shin *et al*., 2014), which describes an instantaneous rise to the maximum overpressure followed by an exponential decay to ambient pressure, or with further simplified triangular loading function based on empirical charts available in many textbooks and US government-published documents such as Smith and Hetherington (1994), UFC 3-340-02 (DoD 2008), Cormie *et al.* (2009), ASCE (2010) and Dusenberry (2010). These empirical charts provide air-blast parameters such as incident and reflected peak overpressures and scaled impulses, positive phase duration, and shock front velocity for spherical free-air bursts and hemispherical surface bursts. Also, UFC 3-340-02 presents charts for reflected overpressures and impulses varying angle of incidence. Computer codes such as ConWep (Hyde, 1992) implement these empirical relationships and are widely used for design of protective structures.

The SDOF elastic-plastic charts in UFC 3-340-02 provide maximum displacements of the system and the corresponding times as a function of two non-dimensional variables of t_d/T_n and R_{me}/F_e, where t_d is loading duration, T_n is natural period, R_{me} is equivalent maximum resistance, F_e is equivalent load. However, the charted data are insufficient to obtain the responses in the near field. The minimum T_d/T_n and R_{me}/F_e in the charts are 0.1 and 0.1, respectively, but in the near and intermediate fields, both variables are beyond these ranges unless the structural components are unrealistically stiff, which is discussed in detail in Section 2. Accordingly, for adequate evaluation of the SDOF elastic-plastic approach for close-in detonations, the existing charts need to be extended with much greater range of t_d/T_n and R_{me}/F_e.

The SDOF analysis and the corresponding charts available in

*Research Professor, Dept. of Architectural Engineering, Dankook University, Yongin 16890, Korea (E-mail: jshin@dankook.ac.kr)
**Member, Associate Professor, Dept. of Architectural Engineering, Dankook University, Yongin 16890, Korea (Corresponding Author, E-mail: kklee@dankook.ac.kr)

Biggs (1952), UFC 3-340-02 (DoD, 2008), ASCE (2010) and others, as described previously, requires a plane shock wave with an assumption of blast overpressures loaded uniformly to structures. This has been considered appropriate for the far-field detonations. However, one may call into question the use of the SDOF method for the near-field detonations because the overpressures acing on structures will vary significantly with distance and angle of incidence, which indicates that the SDOF method can significantly overpredict the responses of structures, noting that the near-field effect has not been reflected in the SDOF analysis. The near field is defined herein as regions for scaled distances, Z, of approximately less than 0.8 m/kg$^{1/3}$ (Shin *et al.*, 2015), where $Z = R/W^{1/3}$, where R is distance and W is charge weight. Beyond this range, the uniform and non-uniform blast loads lead to similar responses of structures, which will be shown later in this paper.

In this paper, SDOF calculations are first performed to generate the maximum responses associated with the near field and to evaluate the utility of the SDOF charts with a focus on the near field. These calculations are conducted using the central difference method (CDM) (e.g., Chopra, 2012), and the results are verified with comparison to those presented in UFC 3-340-02 (DoD, 2008) for far-field detonations and those obtained performing a three-dimensional finite element analysis for near-field detonations. Once confirming the accuracy of the calculations, they are further examined numerically to study the near-field effects on the responses of structures.

A sample steel component subjected to blast loading is simulated using LS-DYNA (LSTC, 2013) to evaluate the applicability of the updated charts, especially to near-field detonations. Three loadings I, II and III with identical reflected impulses are considered. Loadings I is a uniform triangular loading used in the SDOF charts developed in this study. Loading II and III are uniform and non-uniform ConWep reflected overpressure histories, respectively. A discussion for the selection of these loadings is provided later in Section 5. Only positive phases of these loadings are considered noting that the negative phase has been known to have an insignificant effect on the structural responses. Results are discussed, and recommendations and limitations for the SDOF elastic-plastic analysis and charts are provided with an emphasis on the near field.

2. Inelastic SDOF Approach for Blast-resistant Design

Figure 1 describes a typical equivalent SDOF analysis. Blast pressure loads by far-field detonations are assigned uniformly on

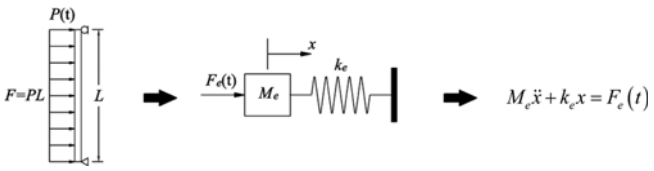

Fig. 1. Equivalent SDOF Analysis

Table 1. Transformation Factors, Maximum Resistance and Stiffness for Simply Supported Beam (UFC 3-340-02 (DoD, 2008))

Strain rage	Elastic	Plastic
Load factor, K_L	0.64	0.50
Mass factor, K_M	0.50	0.33
Maximum resistance, R_m	8 M_p/L	8 M_p/L
Stiffness, k	$384EI/5L^3$	-

structures. A simply-supported beam, column, or slab subjected to these uniform blast loads is transformed into an equivalent SDOF system. The equivalent load, F_e, equivalent mass, M_e, and equivalent stiffness, k_e, of the SDOF system are obtained using transformation factors available in UFC 3-340-02 (DoD, 2008). Table 1 shows these transformation factors for mass, K_M, and load, K_L, and the maximum resistance, R_m, and stiffness, k, for simply-supported condition. The load transformation factor is also used to compute the equivalent maximum resistance, R_{me}, and the equivalent stiffness, k_e. An equation of motion is accordingly derived from the equivalent SDOF system. Damping for the high-frequency and short-duration shock loadings is ignored (Biggs, 1964).

Structures are assumed to show elastic-perfectly plastic deformation. Fig. 2(a) shows the resistance function. UFC 3-340-02 (DoD, 2008) provides elastic-plastic SDOF charts for rectangular and triangular loads, where the latter, as shown in Fig. 2(b), is often used for simplified blast load (e.g., Jones *et al.*, 2009) because the loading is similar in shape to blast loads and is thus adopted in this study. The negative phase of the resistant function is not considered because the maximum responses of the system occur in the positive-phase direction, which is consistent with UFC 3-340-02 (DoD 2008). Fig. 3 presents the UFC 3-340-02 charts for the maximum responses of elastic-plastic SDOF system under triangular loading. These charts are digitized for verification of SDOF elastic-plastic calculations presented in Section 3.

The charts presented in Fig. 3 are widely used for calculations of the maximum responses of structures to impulsive loadings. However, these data are insufficient to obtain the responses for near-field detonations. Consider a A36 steel component with dimensions of 0.2 × 0.2 × 4 m designed to have a plastic section modulus similar to one of the standard steel section W14 × 74

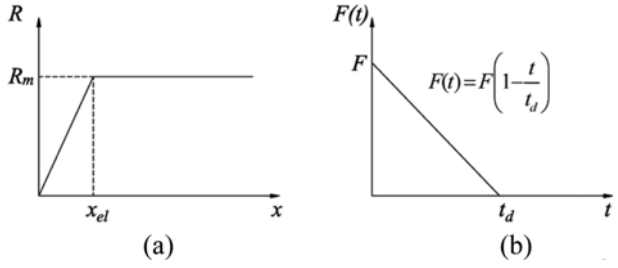

Fig. 2. Resistance Function and Triangular Pulse: (a) Resistance Function, (b) Triangular Pulse

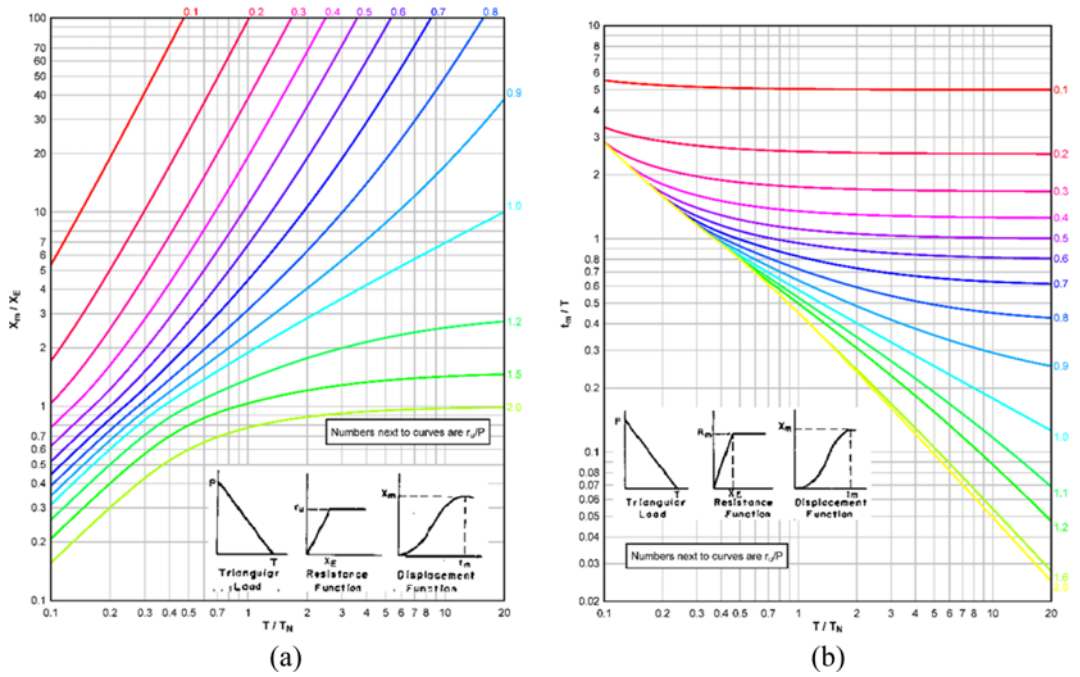

Fig. 3. Maximum Responses of Elastic-plastic SDOF System Subjected to Triangular Loading (UFC 3-34-02 (DoD, 2008)): (a) x_m/x_{el} (x_m/x_E in the chart), (b) t_m/t_d in the chart)

and a typical slab-to-slab height of 4 m. The static yield stress of the A36 steel of 252.2 MPa (36.58 ksi) is chosen per UFC 3-340-02. The effect of strain rate, which is generally considered for blast analysis, is realized using the Dynamic Increase Factor (DIF) of 1.36. UFC 3-340-02 reports this value for A36 steel with flexure and high pressure range such that the dynamic yield stress of approximately 350 MPa is used in this study. The maximum resistance, R_m, is thus calculated as 1,400 kN and the stiffness, k, is 32,000 kN/m per Table 1. The equivalent maximum resistance, R_{me}, and the equivalent stiffness, k_e, are computed using the load transformation factors, as shown in Table 1. The natural period, T_n, is then computed as 0.0335 seconds for a density of 7,830 kg/m^3 and the elastic modulus of 200 GPa, which yields Fig. 4 that presents R_{me}/F_e and t_d/T_n as a function of scaled distance, Z, for a hand-delivered explosive of TNT of 20 kg, noting that $t_d = 2\ I_r/P_r$ for triangular pulse. The reflected impulse, I_r, and the reflected peak overpressure, P_r, for the given scaled distances are obtained from UFC 3-340-02. Fig. 4 shows that values of R_{me}/F_e and t_d/T_n associated with the near field are below the lower bounds provided in the UFC 3-340-02 charts (0.1 and 0.1, respectively, see Fig. 3), which are associated with the range $Z < 0.67$ m/kg$^{1/3}$ for R_{me}/F_e and the range $Z < 2.8$ m/kg$^{1/3}$ for t_d/T_n. This is explained in more detail using the following relationships.

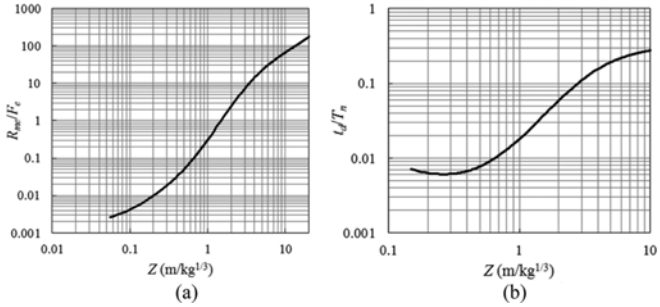

Fig. 4. Variables of Elastic-plastic SDOF Charts (R_{me}/F_e and t_d/T_n) in UFC 3-340-02 as a Function of Scaled Distance for a Steel Component: (a) R_{me}/F_e, (b) t_d/T_n

Relationships between R_{me}/F_e and the properties of the steel component are expressed as:

$$\frac{R_{me}}{F_e} = \frac{K_L 8M_p/l_h}{K_L P_r l_w l_h} = \frac{2F_y}{P_r} \times \left(\frac{l_t}{l_h}\right)^2 \quad (1)$$

where M_p is plastic moment, l_h, l_w and l_t are height, width and thickness, respectively, P_r is reflected peak overpressure, and F_y is yield strength. To maintain R_{me}/F_e greater than 0.1, l_t/l_h needs to be significantly increased, which indicates that for near-field detonations, the SDOF charts can be used only for excessively stiff steel components.

For t_d/T_n, the following relationship is obtained:

$$\frac{t_d}{T} = \frac{2I_r/P_r}{2\pi\sqrt{\frac{m_e}{k_e}}} = \frac{2(I_r/W^{1/3})/P_r}{2\pi\sqrt{\frac{m_e}{k_e}}} \times W^{1/3} \quad (2)$$

where I_r is reflected impulse, m_e is equivalent mass, k_e is equivalent stiffness, and W is charge weight. For the given steel component and scaled distance, t_d/T_n is proportional only to $W^{1/3}$ and is expressed as t_d/T_n = constant × $W^{1/3}$, noting that $I_r/W^{1/3}$ is invariable for a certain scaled distance per UFC 3-340-02. In Fig. 4(b), since the minimum value of t_d/T_n is approximately 0.006, for a

given scaled distance, the charge weights should be increased by a factor of approximately 17^3 or greater to shift the lower bound of t_d/T_n from 0.006 to more than 0.1, thereby utilizing the UFC charts for all range of scaled distance. Accordingly, the UFC elastic-plastic SDOF charts need to be generated for greater range of R_{me}/F_e and t_d/T_n.

3. SDOF Elastic-plastic Response Calculations

A SDOF calculations with elastic-perfectly plastic resistance are performed to obtain the results for the smaller values of t_d/T_n and R_{me}/F_e. The associated resistance function and equation of state are established, and they are solved numerically using the central difference method (CDM, Chopra, 2012). The two non-dimensional quantities of t_d/T_n and F_{me}/F_e are extended down to 0.001 and 0.001, respectively, which will cover the region close to the charge face (see Fig. 4). The SDOF-calculated results are verified using the UFC 3-340-02 charts for relatively larger values of t_d/T_n and R_{me}/F_e, namely, far-field detonations. For smaller values of t_d/T_n and R_{me}/F_e, namely, near-field detonations, a finite element analysis is performed for the verification.

3.1 Resistance Functions and Triangular Loading

The relationship between the resistance, R, and the displacement, x, for elastic-plastic system is expressed using a bilinear function (see Fig. 2(a)). The peak responses occur within the two stages assuming that only positive phase of loading is considered. The resistance, $R(x)$, as a function of displacement, x, is thus given by:

$$R(x) = \begin{cases} k_e x & \text{for} \quad 0 < x < x_{el} \\ R_{me} & \text{for} \quad x_{el} < x < x_m \end{cases} \tag{3}$$

where k is equivalent stiffness, R_{me} is equivalent maximum resistance, x_{el} is yield displacement, and x_m is maximum displacement. The triangular loading history, $F(t)$, is defined as (see Fig. 2(b)):

$$F(t) = \begin{cases} F_e\left(1 - \dfrac{t}{t_d}\right) & \text{for} \quad t < t_d \\ 0 & \text{for} \quad t > t_e \end{cases} \tag{4}$$

where F is equivalent peak load, and t_d is positive phase duration.

3.2 Numerical Calculations

Equations of motion are constructed for two cases: 1) when t_{el} is smaller than t_d and 2) when t_{el} is greater than t_d. The effect of damping is neglected (typically for blast analysis), as described previously. The initial conditions for displacement, velocity and acceleration are assumed zero.

Figure 5 describes a scheme to establish an equation of motion when $t_{el} < t_d$. The equations of motion are built in three steps:

$$\begin{aligned} &m_e\ddot{x}(t) + k_e x(t) = F(t) \quad \text{for} \quad x < x_{el} \quad \text{and} \quad t < t_{el} < t_d \\ &m_e\ddot{x}(t) + R_{me} = F(t) \quad \text{for} \quad x < x_{el} \quad \text{and} \quad t_{el} < t < t_d \\ &m_e\ddot{x}(t) + R_{me} = 0 \quad \text{for} \quad x < x_{el} \quad \text{and} \quad t_{el} < t_d < t \end{aligned} \tag{5}$$

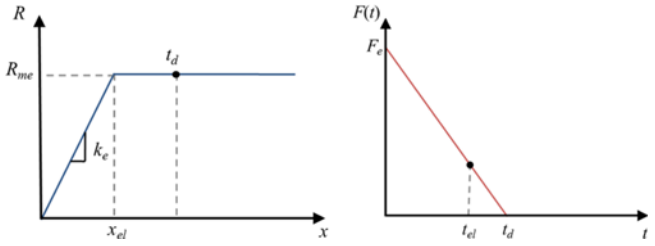

Fig. 5. When $t_{el} > t_d$

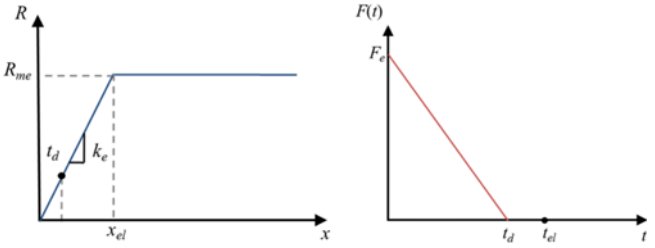

Fig. 6. When $t_{el} < t_d$

Equations of motion for $t_{el} > t_d$, are constructed similarly in three steps based on the scheme described in Fig. 6:

$$\begin{aligned} &m_e\ddot{x}(t) + k_e x(t) = F(t) \quad \text{for} \quad x < x_{el} \quad \text{and} \quad t < t_d \\ &m_e\ddot{x}(t) + k_e x(t) = 0 \quad \text{for} \quad x < x_{el} \quad \text{and} \quad t_d < t < t_{el} \\ &m_e\ddot{x}(t) + R_{me} = 0 \quad \text{for} \quad x > x_{el} \quad \text{and} \quad t_{el} < t \end{aligned} \tag{6}$$

These constructed equations of motion are solved numerically using CDM. Fig. 7 presents the updated charts developed for t_d = 0.1 sec, F_e = 1 kN, and m_e = 1 kg, where the rectangular dashed lines indicates the ranges of the UFC 3-340-02 charts. These SDOF calculations are verified using the UFC 3-340-02 charts and through finite element analysis in the following section.

4. Verification of SDOF Calculations

4.1 Verification using UFC 3-340-02 Charts

Figure 8 enables a comparison of UFC 3-340-02 (DoD, 2008) predictions and SDOF calculations in Section 3.2 for triangular loading in the range $0.1 < t_d/T_n < 20$ and $0.1 < R_{me}/F_e < 2$, where t_d/T_n of 0.1 corresponds to Z = 2.8 m/kg$^{1/3}$ (see Fig. 4(b)). The UFC predictions and the SDOF calculations are in excellent agreement for both x_m/x_{el} and t_m/t_d, as shown in Fig. 8. The algorithms of the calculations are thus considered verified in the far-field range.

4.2 Verification using Finite Element Analysis

Three-dimensional (3D) finite element analysis is performed using LS-DYNA (LSTC, 2013) to further verify the SDOF calculations in the near-field range. A simply-supported sample A 36 steel component with dimensions of 0.2 × 0.2 × 4 m is designed to have a plastic section modulus similar to W14 × 74 and is modeled using 20,000 eight-node solid elements, where the element size is 0.02 × 0.02 × 0.02 m and this size is considered

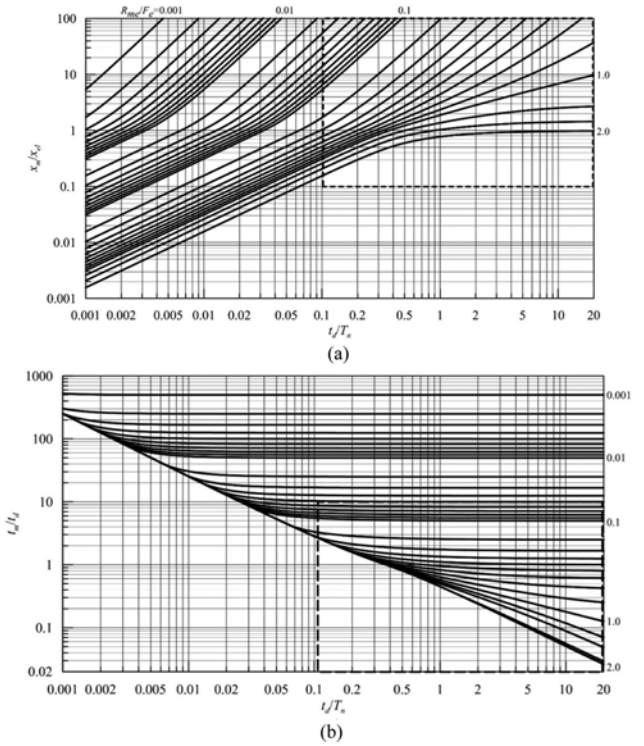

Fig. 7. Updated Charts for Maximum Response of Elastic-plastic SDOF System for Triangular Loading: (a) x_m/x_{eL}, (b) t_m/t_d

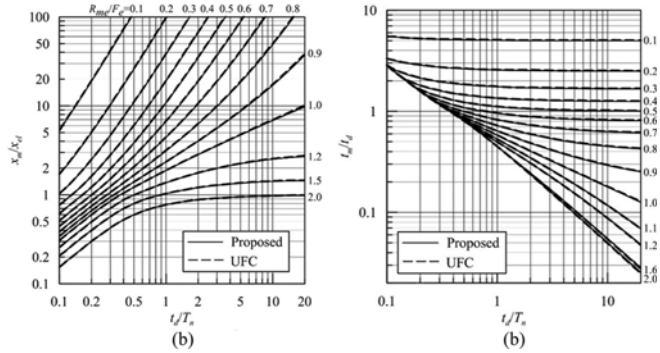

Fig. 8. Verification of Proposed Charts Using the UFC 3-340-02 Charts: (a) x_m/x_e, (b) t_m/t_d

sufficiently small to obtain mesh convergence. The element formulation for the solid elements are taken as under-integrated constant stress. Hourglass control reported by Belytschko and Binderman (1993) that invokes an assumed-strain co-rotational formulation for the under-integrated solid elements is used.

The A36 steel components with the elastic modulus of 200 GPa and the density of 7,860 kg/m^3, as described previously, are modeled with MAT_PLASTIC_KINEMATIC. The dynamic yield stress of 350 MPa with consideration of strain-rate effects for blast events, as described in Section 2, is used for analysis.

The blast loading is assumed as a triangular pulse, as shown in Fig. 2(b), for purpose of comparison to the SDOF calculations achieved in Section 3 and is uniformly distributed on the steel component, as shown in Fig. 9. The reflected peak overpressure,

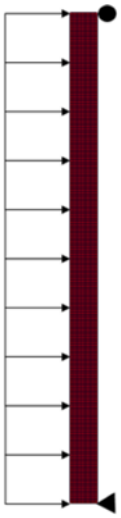

Fig. 9. 3D FE model of Steel Component under Uniform Triangular Pulse

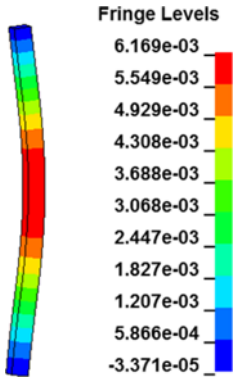

Fig. 10. Maximum Displacement Contour for Z = 1 m/kg$^{1/3}$

P_r, and the reflected impulse, I_r, for a given scaled distance are determined per UFC 3-340-02 (DoD, 2008) for a spherical TNT explosion in free air at sea level. The positive phase duration for the triangular pulse is calculated as $2I_r/P_r$.

Analysis is conducted for eight scaled distances, Z, of 0.15, 0.2, 0.3, 0.4, 0.6, 0.8, 1 and 2 m/kg$^{1/3}$. The lower limit on Z of 0.15 m/kg$^{1/3}$ is chosen because ConWep (or data in UFC 3-340-02) provides overpressure histories at Z > 0.147 m/kg$^{1/3}$. The upper limit on Z of 2 m/kg$^{1/3}$ is based on t_d/T_n of 0.1 corresponding to Z = 2.8 m/kg$^{1/3}$, as shown in Fig. 4(b). Fig. 10 shows the simulation result for Z = 1 m/kg$^{1/3}$ in the moment that the steel component reaches the maximum displacement.

Figure 11 presents results for x_m/x_{el} and t_m/t_d. The results analyzed using LS-DYNA in 3D and the 1D numerical calculations described in Section 3.2 are virtually identical, indicating the algorithms of the SDOF calculations and the results are considered verified for near-field detonations.

5. Responses of Steel Components for Near-field Detonations

The sample steel component representing W14 × 74, as introduced

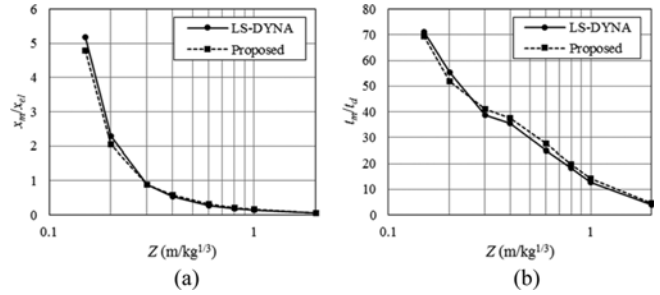

Fig. 11. Verification of Proposed SDOF Calculations Through Finite Element Analysis: (a) x_m/x_{el}, (b) t_m/t_d

in Section 4, subjected to blast loading is further simulated in LS-DYNA (LSTC, 2013) to examine the applicability of the SDOF analysis using uniform load to the near field. Eight scaled distances of Z = 0.15, 0.2, 0.3, 0.4, 0.6, 0.8, 1 and 2 m/kg$^{1/3}$, adopted in Section 4, are also used here for the similar reason. Three loadings with similar reflected impulses are considered: loading I (uniform triangular), loading II (uniform ConWep), and loading III (non-uniform ConWep). Loading I is that used in UFC 3-340-02 (DoD, 2008) and is a simplified form of Friedlander-shaped loading II with the assumption of the uniform load on the steel component, as described previously. Loading III involves the effects of pressure decrease due to the distance and the angle of incidence.

5.1 Blast Loadings

Figure 12 shows the blast loading (reflected overpressure and the corresponding impulse) histories at Z = 0.2 m/kg$^{1/3}$. The uniform triangular loading (I) is that used in the SDOF calculations in Sections 3 and 4. The uniform ConWep loading (II) uses a Friedlander-shaped reflected overpressure history for normal incidence, which is uniformly distributed on the front face of the steel component. Note that data in UFC 3-340-02 for air-blast parameters have been implemented in ConWep. The non-uniform ConWep loading (III) uses reflected overpressure histories estimated along the front face of the steel component with consideration of standoff distance and angle of incidence. The data source is same as the loading II. The ConWep loadings associated loadings II and III for spherical free-air burst are

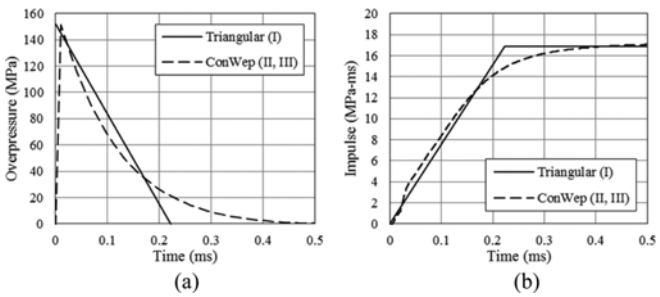

Fig. 12. Triangular and ConWep Reflected Overpressure and Reflected Impulse Histories at Z = 0.2 m/kg$^{1/3}$: (a) Over-Pressure, (b) Impulse

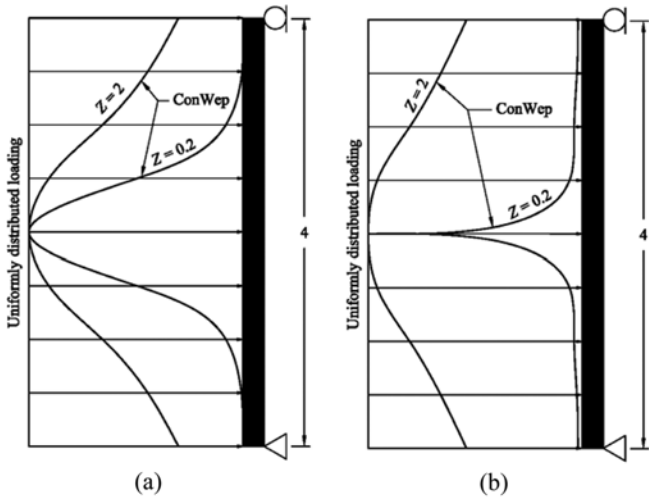

Fig. 13. Normalized Pressure and Impulse Distributions on a Steel Component with a Height of 4 m (Z in units of m/kg$^{1/3}$): (a) Normalized Pressure, (b) Normalized Impulse

implemented using LOAD_BLAST_ENHANCED in LS-DYNA. These three overpressure histories are applied to the sample steel component.

Figure 13 enables a comparison of pressure and impulse distributions along the 4 m-height steel component between uniformly distributed loading and non-uniform loadings for Z = 0.2 and 2 m/kg$^{1/3}$. The non-uniform loading is generated using ConWep. The pressures and impulses are normalized by the peak values to observe the uniformity varying scaled distance. As scaled distance decreases, the difference of pressure and impulse between uniform and non-uniform (ConWep) loadings near the center of the component increases, indicating the use of uniform loading in the near field can significantly overpredict the responses of structures.

5.2 Results

Numerical responses of the steel component subjected to the three blast loadings for Z = 0.15, 0.8, 1 and 2 m/kg$^{1/3}$ are presented in Fig. 14. The uniform triangular (I) and uniform ConWep (II) loadings lead to similar results for all considered scaled distances, as predicted. The results also enables investigation on the limitation for the use of uniform blast loads in the near field. For intermediate or far field, namely, Z = 1 and 2 m/kg$^{1/3}$, the peak displacements and the time to the peaks are similar for all three loadings. The differences are less than 10%, which is satisfactory for the purpose of design. In the near field, namely, $Z \leq 0.8$ m/kg$^{1/3}$, the peak displacement for non-uniform ConWep loading (III) are significantly less than those for uniform loadings (uniform triangular (I) and uniform ConWep (II)). This difference increases as scaled distance decreases. These observations indicate that the current approach for SDOF analysis and design charts described previously are appropriate in the range Z > 1 m/kg$^{1/3}$. For $Z \leq 0.8$ m/kg$^{1/3}$, the charts may significantly overpredict responses of structures.

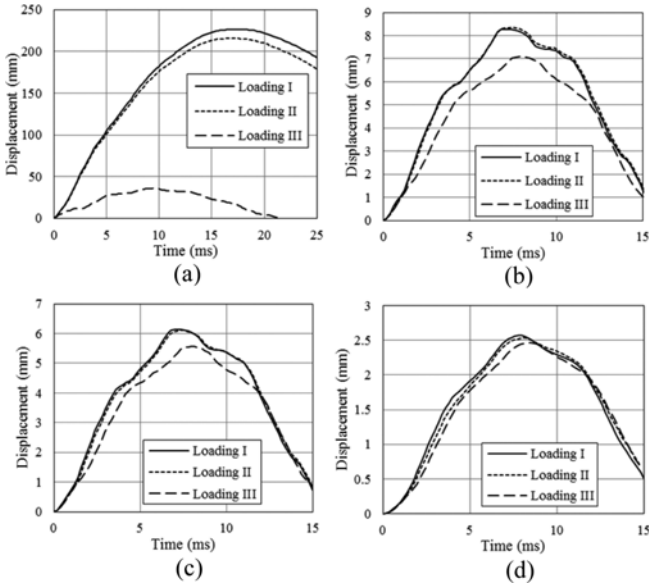

Fig. 14. Displacement Histories of a Steel Component Subjected to Various Loading Types: (a) Z = 0.15 m/kg$^{1/3}$, (b) Z = 0.8 m/kg$^{1/3}$, (c) Z = 1 m/kg$^{1/3}$, (d) Z = 2 m/kg$^{1/3}$

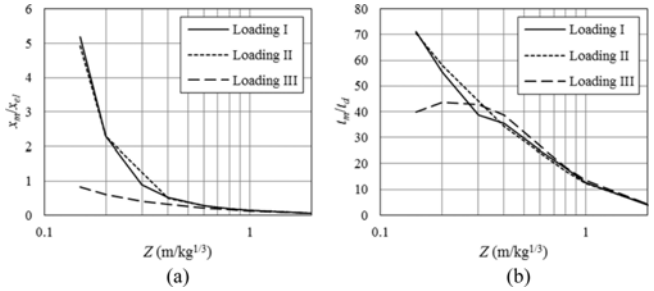

Fig. 15. Responses of a Steel Component as a Function of Scaled Distance: (a) x_m/x_{el}, (b) t_m/t_d

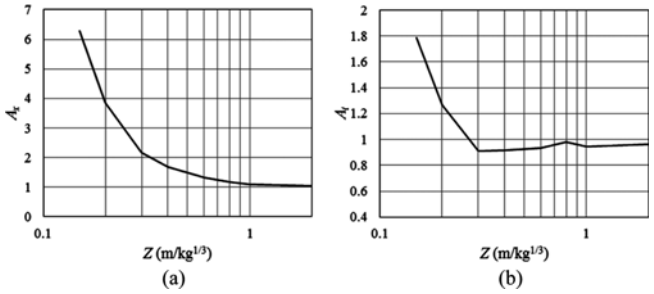

Fig. 16. Adjustment Factors of A_x and A_t as a Function of Scaled Distance: (a) A_x, (b) A_t

Figure 15 presents ratios of maximum to yield displacement (x_m/x_{el}) and of time to the maximum displacement to positive phase duration (t_m/t_d) as a function of scaled distance for the three loadings. Differences between the displacement ratios for uniform and non-uniform loadings are observed at approximately Z < 0.8 m/kg$^{1/3}$, as described previously. For time ratio, the differences are identified at approximately Z < 0.3 m/kg$^{1/3}$.

For this limited case of the steel component representing W14 × 74, adjustment factors are provided, as presented in Fig. 16. The adjustment factor for maximum displacement (A_x) is the ratio of maximum displacement (x_m) for uniform triangular loading (I) to that for non-uniform ConWep loading (III). The adjustment factor for maximum response time (A_t) is the ratio of maximum response time (t_m) for uniform triangular loading (I) to that for non-uniform ConWep loading (III). Fig. 16(a) shows that, for the smallest scaled distance of 0.15 m/kg$^{1/3}$ considered in this study, the current SDOF approach overpredicts the maximum displacement by a factor of approximately 6. These adjustment factors will have to be considered for the purpose of optimal design.

6. Conclusions

This paper presents numerical calculations to obtain the maximum responses of the elastic-plastic SDOF system for scaled distances between 0.15 and 2 m/kg$^{1/3}$. The limitations and recommendations for the SDOF analysis are discussed with a focus on the near field. The near-field effect associated with non-uniform loading on the responses of structures has been studied.

The elastic-plastic SDOF charts presented in UFC 3-340-02 are insufficient to obtain the responses for near-field detonation. The lower limits of two dimensionless key parameters of t_d/T_n and R_{me}/F_e were thus extended from 0.1 and 0.1, respectively, to 0.001 and 0.001 using numerical algorithms. The results have been verified successfully for far-field detonations using the UFC 3-340-02 charts and for near-field detonations through finite element analysis.

The current SDOF elastic-plastic design approach may be inappropriate for near-field detonations, namely, Z < 0.8 m/kg$^{1/3}$ because the use of the uniform load is not adequate in this range where the effects of distance and angle of incidence produce the very large non-uniformity of blast load. For reasonable evaluation of structures in this near field, the effect of non-uniform loads considering distance and angle of incidence should be addressed.

For a limited case of a steel component representing W14 × 74, factors to adjust the maximum responses in the existing SDOF elastic-plastic approach are provided. The maximum displacement and corresponding time of a structural component under near-field detonation resulting from the SDOF chart shall be divided by the adjustment factors, respectively. These factors will be useful to remedy the shortcomings of the SDOF elastic-plastic charts for near-field detonations, noting that the adjustment factors for alternate steel components can be possibly different from those provided in this study.

Acknowledgements

The present research was conducted by the research fund of Dankook University in 2015.

References

ASCE Task Committee on Blast-Resistant Design (2010). *Design of*

blast-resistant buildings in petrochemical facilities, 2nd Ed. Americal Society of Civil Engineers, Reston, VA.

Baker, W. E. (1973). *Explosions in air*, University of Texas Press, Austin and London.

Belytschko, T. and Bindeman, L. P. (1993). "Assumed strain stabilization of the eight node hexahedral element." *Computer Methods in Applied Mechanics and Engineering*, Vol. 105, No. 2, pp. 225-226, DOI: 10.1016/0045-7825(93)90124-G.

Biggs, J. M. (1964). *Introduction to structural dynamics*, McGraw-Hill, NY.

Chopra, A. K. (2012). *Dynamics of structures: Theory and applications to earthquake engineering, 4th edition*, Prentice Hall, Upper Saddle River, NJ.

Cormie, D., Mays, G., and Smith, P. (2009). *Blast effects on buildings, 2nd Ed*. London: Thomas Telford.

Department of the Army, Navy and Air Force (1990). *Structures to resist the effects of accidental explosions (with Addenda)*, Army Technical Manual (TM 5-1300), Navy Publication (NAVFAC P-397), Air Force Manual (AFM 88-22), Revision 1. Washington, DC.

Department of defence (2008). *Unified Facilities Criteria (UFC): Structures to Resist the Effects of Accidental Explosions (UFC 3-340-02)*. Departments of Defense, Washington, DC.

Dusenberry, D. O. (2010). ed. *Handbook for blast-resistant design of buildings*, Wiley, Hoboken, NJ.

Jones, J., Wu, C., Oehlers, D. J., Whittaker, A. S., Marks, S., and Coppola, R. (2009). "Finite difference analysis of simply supported RC slabs for blast loadings." *Engineering Structures*, Vol. 31, No. 12, pp. 2825-2832, DOI: 10.1016/j.engstruct.2009.07.011.

Hyde, D. W. (1992). *ConWep: Conventional weapons effects (Application of TM 5-855-1)*, US Army Corps of Enigneers, Waterways Experiment Station, Vicksburg, MS.

LSTC (2013). *LS-DYNA keyword user's manual Ver. R7.0*. Livermore Software Technology Corporation, Livermore, CA.

Norris, C. H., Hansen, R. J., Holley, JR. M. J., Biggs, J. M., Namyet, S., and Minami, J. K. (1959). *Structural design for dynamic loads*, McGraw-Hill, New York; Toronto; London.

Shin, J., Whittaker, A. S., Aref, A. J., and Cormie, D. (2014). *Air blast effects on civil structures*, Technical Rep. No. MCEER-14-0006, Multidisciplinary Center for Earthquake Research, Univ. at Buffalo, Buffalo, NY.

Shin, J., Whittaker, A. S., and Cormie, D. (2015). "Incident and normally reflected overpressure and impulse for detonations of spherical high explosives in free air." *Journal of Structural Engineering*, Vol. 141, No. 12, 04015057.

Smith, P. D. and Hetherington, J. G. (1994). *Blast and ballistic loading of structures*, Butterworth-Heinemann, Oxford; Boston.